



**HAL**  
open science

## Mineralogical characterization of copper lateritic ore from the Furnas deposit - Carajás, Brazil

Eliana Satiko Mano, Laurent Caner, Sabine Petit, Arthur Pinto Chaves

► **To cite this version:**

Eliana Satiko Mano, Laurent Caner, Sabine Petit, Arthur Pinto Chaves. Mineralogical characterization of copper lateritic ore from the Furnas deposit - Carajás, Brazil. REM - International Engineering Journal, 2020, 73 (3), pp.329-335. 10.1590/0370-44672019730113 . hal-03000975

**HAL Id: hal-03000975**

**<https://hal.science/hal-03000975>**

Submitted on 27 Nov 2020

**HAL** is a multi-disciplinary open access archive for the deposit and dissemination of scientific research documents, whether they are published or not. The documents may come from teaching and research institutions in France or abroad, or from public or private research centers.

L'archive ouverte pluridisciplinaire **HAL**, est destinée au dépôt et à la diffusion de documents scientifiques de niveau recherche, publiés ou non, émanant des établissements d'enseignement et de recherche français ou étrangers, des laboratoires publics ou privés.

# MINERALOGICAL CHARACTERIZATION OF Cu-LATERITIC ORE FROM THE FURNAS DEPOSIT - CARAJÁS, BRAZIL

Eliana Satiko Mano<sup>1\*</sup>, Laurent Caner<sup>2</sup>, Sabine Petit<sup>2</sup> and Arthur Pinto Chaves<sup>1</sup>

<sup>1</sup>*Escola Politécnica - Universidade de São Paulo. Av. Prof. Mello Moraes 2.373 - 05508-900, São Paulo - Brasil. elli\_mano@hotmail.com*

<sup>2</sup>*Institut de Chimie des Milieux et Matériaux de Poitiers, IC2MP, UMR 7285 Université de Poitiers, CNRS - Poitiers, France*

## ABSTRACT

Furnas is a small and not well-known copper sulfide deposit in the northern Carajás mineral province (Pará State, Brazil). Mineralogical and geochemical studies were performed on three weathered samples in order to verify the presence of copper in the lateritic minerals. According to these Cu-bearing minerals, the weathered ore can be exploited. X-ray diffraction (XRD), Scanning Electron Microscopy (SEM) and Fourier Transformed Infrared (FTIR) spectroscopy analyses have shown that the copper is mainly associated to cryptomelane and to clay minerals and, although goethite composes from 40 to 50% of the samples (weight %), less than 0.1% of the total Cu is associated to it. Based on the results, the weathering sequence could be established; the alteration processes were responsible for the dissolution of the copper primary sulfides; the Cu released by these sulfides is, afterwards, incorporated in biotites and vermiculites, following the gneiss schistosity. Afterwards, the biotites altered to an interstratified 10-14 Å and subsequently to an Al-Fe-Cu smectite; finally, smectite was altered to kaolinite and the Cu was leached.

Keywords: Carajás, Furnas deposit, mineral characterization; Cu-bearing minerals, clay minerals.

## 1. INTRODUCTION

The mineral province of Carajás is considered one of the most important iron oxide copper gold ore provinces (IOCG) in the world (Teixeira et al., 2010; Groves et al., 2010), often compared to the Olympic Dam in Australia (Tallarico et al., 2005); it is located in the eastern part of the Amazon craton in northwestern Brazil. The estimated Cu resource for all of the Carajás province is around 2 billion metric tons (Bt), with an average 1.4 wt % of Cu and 0.28 to 0.86 g/t of Au (Moreto et al., 2015), for the sulfide ore.

The Carajás province is formed by two tectonic domains: Carajás and Rio Maria, limited by a regional E-W discontinuity (Monteiro et al., 2014). The Rio Maria domain comprehends greenstone belts of the metavolcanic sediments type and mesoarchean magmatism (granites and granodiorites). In addition, the Carajás domain is formed by mesoarchean magmatism, especially granites, gneisses and metavolcanic sediments, without greenstone belt evidences. The Archean basement is covered by Igarapé Salobo-Pojuca and Grão Pará group sediments (amphibolites, quartzites and banded iron formations - BIFs). Finally, marine and fluvial clastic sediments of the Águas Claras Formation are discordantly deposited above it (Schwarz and Frantz, 2013; Moreto et al., 2015). Lately, intrusions of mafic, ultramafic rocks and granites followed by tectonic events reactivated old faults resulting in low-grade metamorphism (greenschist facies) and metasomatism/hydrothermalism events. These hydrothermal events led to the formation of the primary Cu-sulfide mineralizations. Weathering and hydrothermal alterations of these sulfides lead to the Cu-bearing lateritic minerals formation.

Based on the studies by Oliveira et al. (1995), Toledo-Groke et al. (1987) and Veiga et al. (1991), which described malachite, cryptomelane, goethite and clay minerals as the main Cu-bearing lateritic minerals in the Salobo deposit, a detailed mineralogical study was conducted on the lateritic samples from the Furnas deposit. According to the results, the lateritic ore from Furnas could also be exploited together with the sulfide ore in order to increase the Cu recoveries.

## 2. MATERIALS AND METHODS

Three samples of different Cu contents were provided by the Vale mining company from the Furnas deposit, a small Cu target, located in the northern Carajás province (Pará, Brazil).

The sampling was performed by Vale and, according to the chemical compositions (table 1) they refer to the different horizons in the weathered profile.

The chemical composition for the three samples was determined by X-ray fluorescence (XRF) on powdered bulk samples with Axios Advanced (PANalytical). Loss on ignition (LOI) values of the bulk samples were obtained from 1g of bulk samples dried at 100°C and heated at 1020°C for two hours; afterwards, the samples were left in a desiccator to cool and later weighed (Dean, 1974). Three samples were separated according to their Cu grades: C1 - Low Cu content (<1% of CuO), C2 - intermediate Cu amount (1-1.5% of CuO) and C3 - high Cu grade (>1.5% of CuO).

The samples were treated with a solution of dithionite, tricitrate and sodium bicarbonate (DCB) at 80°C for 45 min. to solubilize the Fe oxi-hydroxides (Mehra and Jackson, 1960). The Cu in solution was determined by ICP to estimate the Cu associated to the Fe oxi-hydroxides, such as goethite.

The mineralogical assemblage in the bulk samples was identified by randomly oriented X-ray powder diffraction. X-ray diffraction (XRD) patterns were recorded on a Bruker D8 Advance diffractometer (Cu K $\alpha$  radiation - 40 kV, 40 mA- Lynx eye detector) from 2 to 65° 2 $\theta$  with steps of 0.025° 2 $\theta$  and a counting time per step of 115s (converted from scanning mode).

The clay minerals of the samples were studied after the extraction of the <2 $\mu$ m fractions. Initially, the samples were dispersed into distilled water and wet sieved at 50 $\mu$ m. The coarse material (>50 $\mu$ m) was discarded and the fine fractions (<50 $\mu$ m) were saturated with NaCl 1 mol. L<sup>-1</sup> to deflocculate the particles (Moore and Reynolds, 1989). The clay fractions (<2 $\mu$ m) were separated by centrifugation and studied (Mano et al., 2015). Afterwards, the <2 $\mu$ m fraction was separated into five sub-fractions: <0.05 $\mu$ m, 0.05 to 0.1 $\mu$ m, 0.1 to 0.2 $\mu$ m, 0.2-1 $\mu$ m and 1-2 $\mu$ m; each size fraction was studied in detail. The different sub-fractions were separated by successive centrifugation cycles at different relative centrifugal forces (Laird et al., 1991). The bulk <2 $\mu$ m and the sub-micrometric fractions were flocculated, saturated with CaCl<sub>2</sub> 0.5 mol. L<sup>-1</sup> and washed with distilled water by dialysis to remove the excess of salts. XRD patterns were obtained from oriented Ca-saturated clay dried at room temperature (AD) and after ethylene glycol (EG) saturation, from 2 to 50° 2 $\theta$  with steps of 0.025° 2 $\theta$  and a counting time per step of 192 s (converted from scanning mode).

Fourier transformed infrared (FTIR) spectroscopy was used to specify the crystal chemistry of the Cu-bearing clay minerals. Mid infrared analyses (MIR) were performed in transmission mode using a Nicolet Magna-IR 760 spectrometer in the 400-4000 cm<sup>-1</sup> range with a 2 cm<sup>-1</sup> resolution. The spectra were obtained from pressed KBr pellets, prepared by mixing 1 mg of sample with 150 mg of KBr and pressing at 10 t cm<sup>-2</sup> and drying overnight at 110°C. The infra-red spectra were analyzed using the Omnic software.

The <2 $\mu$ m sub-fractions were mounted in polished section slides, coated with metallic carbon to be analyzed in a scanning electron microscopy (SEM) coupled to EDX (energy dispersive X-ray

spectroscopy). The EDX microanalyses were performed both to distinguish the clay minerals composition and to quantify the Cu contents associated to them. The microanalyses were performed on an INCA Energy 300 device from Oxford Instruments, with a Si(Li) detector coupled to a SEM LEO 440 - Leica installed at the Instituto de Geociências at the Universidade de São Paulo - Brazil.

### 3. RESULTS

#### 3.1 Samples composition

According to the XRD and XRF analyses (Table 1), all the three samples exhibited similar mineralogy, essentially composed of quartz, clay minerals and Fe and Mn oxide/hydroxide (goethite and cryptomelane). Sample C1 exhibited larger amounts of quartz than the other samples (30wt%) whereas its contents of goethite and cryptomelane were the lowest (<45% and <3% respectively). Sample C3, on the other hand, exhibited high contents of Fe and Mn oxides/hydroxides (<55% and 10%) and low amounts of quartz (<15%). Sample C2 exhibited an intermediate composition, with nearly 20% of quartz, 50% of goethite and <5% of cryptomelane. For all the samples, the clay mineral contents represented between 20 to 30% (wt%). In the Furnas deposit, the goethite contents vary between 40 and 55% of the bulk samples. Manganese and copper contents showed the same behavior, suggesting that part of the Cu was associated to Mn as cryptomelane.

Table 1 - Chemical composition of the samples (oxides weight %).

Samples	C1	C2	C3
MgO	1.93	1.60	1.36
Al <sub>2</sub> O <sub>3</sub>	9.04	8.68	8.73
SiO <sub>2</sub>	37.0	28.6	24.0
K <sub>2</sub> O	3.12	2.90	2.11
MnO	0.52	1.06	2.22
Fe <sub>2</sub> O <sub>3</sub>	37.8	45.8	47.3
CuO	0.79	1.30	1.69
LOI	8.84	9.50	11.69
total	99.0	99.4	99.1

#### 3.2 Clay minerals study

The XRD patterns of the <2µm Ca-saturated fractions of the three samples (Figure 1), exhibited peaks at  $d_{001AD}=7.1\text{Å}$  and  $d_{002AD}=3.6\text{Å}$  which did not swell after EG treatment, being attributed to kaolinite. Peaks at  $d_{001AD}=10.0\text{Å}$ ,  $d_{002AD}=5.0\text{Å}$  and  $d_{003AD}=3.4\text{Å}$ , which did not shift after EG treatment indicated the presence of mica-illite. Finally, a peak at  $d_{001AD}=14.4\text{Å}$ , which displaced to  $d_{001EG}=15.6$  to  $16.5\text{Å}$  after EG treatment, revealed the presence of swelling clay minerals such as smectite. Figure 1B detailedly showed a low-angle shoulder at  $d_{001EG}=11.6\text{Å}$ , particularly for sample C3, highlighted after the EG solvation. This reflection is attributed to an interstratified clay mineral containing mica and an expandable layer (10Å-14Å). A small amount of vermiculite was also observed in sample C3, thanks to the reflection at  $14.6\text{Å}$  (Figure 1B), which did not shift after EG treatment.

The finest fractions (<0.05 and 0.05-0.1µm), which represent from 15 to 20% (wt%) of the samples, concentrated smectite; while the coarsest fractions (0.1-2µm), which vary from 5 to 10 wt% of the samples, concentrated mica, kaolinite and mixed layers (Figure 2). Samples C1 and C2, in the fractions between 1 and 2 µm, exhibited a  $d_{001}$  at  $12.4\text{Å}$  that displaced to  $12.9\text{Å}$  after EG solvation (Figure 2D), indicating an interstratification of mica and an expandable layer. This mixed layer is almost absent in sample C3, as noticed in Figure 2D.

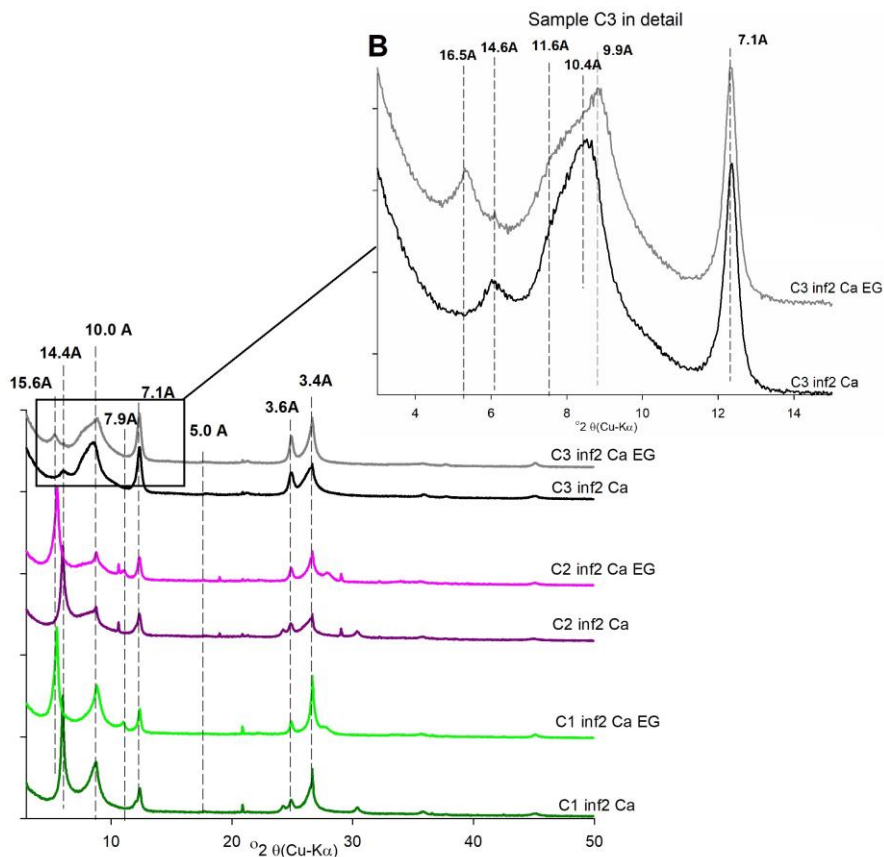


Figure 1 - X-ray diffraction patterns for the blended samples saturated with Ca and after ethylene glycol (EG) solvation. Sample C3 is shown in detail – B

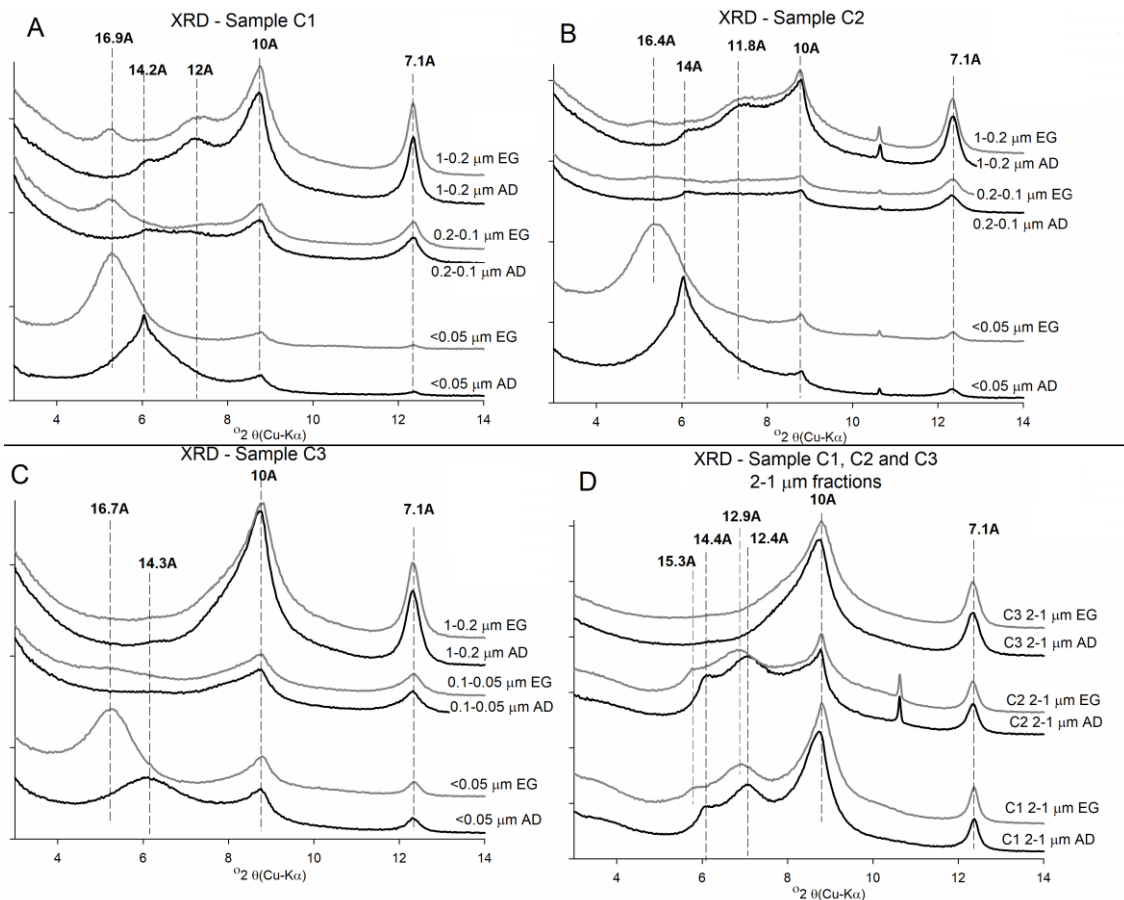


Figure 2 - X-ray diffraction patterns for the three samples C1, C2 and C3 (A, B and C) in air-dried (AD) and after ethylene glycol solvation (EG). Figure D compares the coarse fraction of the three samples

### 3.2.1 Scanning electron microscopy and X-ray dispersion energy analyses

EDX microanalyses for the <2  $\mu\text{m}$  size fractions of samples C1, C2 and C3 confirmed the presence of clay minerals with a composition varying between biotite and smectite, as shown in the ternary diagram  $\text{Al}_2\text{O}_3/\text{K}_2\text{O}/\text{Fe}_2\text{O}_3+\text{CuO}+\text{MgO}$  (Figure 3). The microanalyses data plotted in a ternary diagram of  $\text{MgO}/\text{Al}_2\text{O}_3/\text{Fe}_2\text{O}_3$  confirmed that smectites in the <0.05  $\mu\text{m}$  size fractions have a composition close to nontronite (Figure 3B).

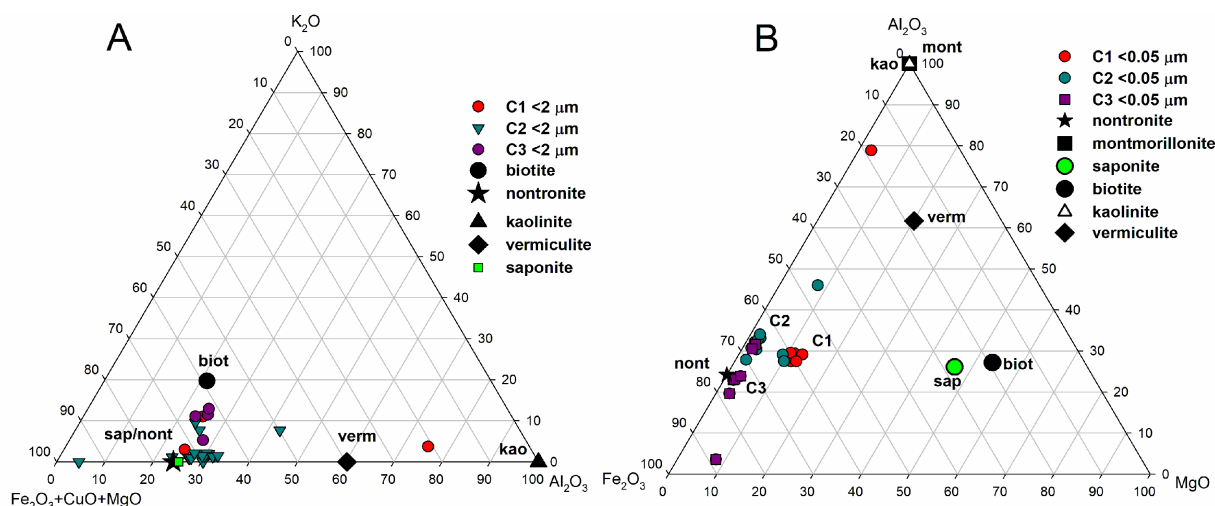


Figure 3 - Ternary diagram for clay mineral particles <2  $\mu\text{m}$  for all samples (A). The theoretical compositions for biotite, nontronite, kaolinite and vermiculite have also been plotted. B - Ternary diagram of <0.05  $\mu\text{m}$  size fraction for all samples. Their composition is close to a Fe-rich dioctahedral smectite (Petit et al., 1992)

### 3.2.2 Mid infrared results

Kaolinite was easily identified in the MIR spectra of all size fractions (Figure 4), especially for the 0.1 - 2  $\mu\text{m}$  size fractions through its characteristic  $\text{AlAlOH}$  stretching bands ( $\nu\text{AlAlOH}$ ) at  $3695\text{ cm}^{-1}$ ,  $3669\text{ cm}^{-1}$ ,  $3653\text{ cm}^{-1}$  and  $3620\text{ cm}^{-1}$  (Farmer, 1974; Madejová et al., 2011). Moreover, the band at  $3596\text{ cm}^{-1}$ , attributed to  $\nu\text{AlFe}^{3+}\text{OH}$  in kaolinite (Petit and Decarreau, 1990; Iriarte et al., 2005), showed that kaolinite contains structural iron.

The broad absorption band centered at  $3420\text{ cm}^{-1}$ , due to water, revealed the presence of smectites. This band is more intense for the <0.05  $\mu\text{m}$  fractions. The observed band at about  $3570\text{ cm}^{-1}$  in the OH stretching region at 820 and  $876\text{ cm}^{-1}$  in the OH bending region allowed characterizing iron rich-smectite and, more precisely, Al-nontronite (Petit et al., 2015). There are three possibilities for copper occupation in smectites: i) in vacant sites of octahedral sheets; ii) in hexagonal cavities of the tetrahedral sheets; iii) as exchangeable  $\text{Cu}^{2+}$  ion in interlayer sheets. Madejová et al. (1999) and Seiffarth and Kaps (2009) described some changes in Si-O vibrations in the MIR region induced by Cu migration in smectites structures. Seiffarth and Kaps (2009) observed a shift from  $1050$  to  $1058\text{ cm}^{-1}$  of Si-OH stretching band resulting from the Cu migration from the interlayer to the hexagonal cavities of the tetrahedral sheet or to octahedral sites.

Petit et al. (1995) demonstrated that the presence of copper induced changes in absorption bands, such as broadening and loss of resolution of the  $3668\text{ cm}^{-1}$ , for synthetic kaolinites, containing from 0.1 to 7% of Cu. In these synthetic samples, copper was suspected to be in the trioctahedral distribution.

The FTIR spectra of the three samples did not show any evidence of the presence of Cu in either the smectite or the kaolinite structure. These features might be due to the too low Cu amounts in the clay minerals to be detected.

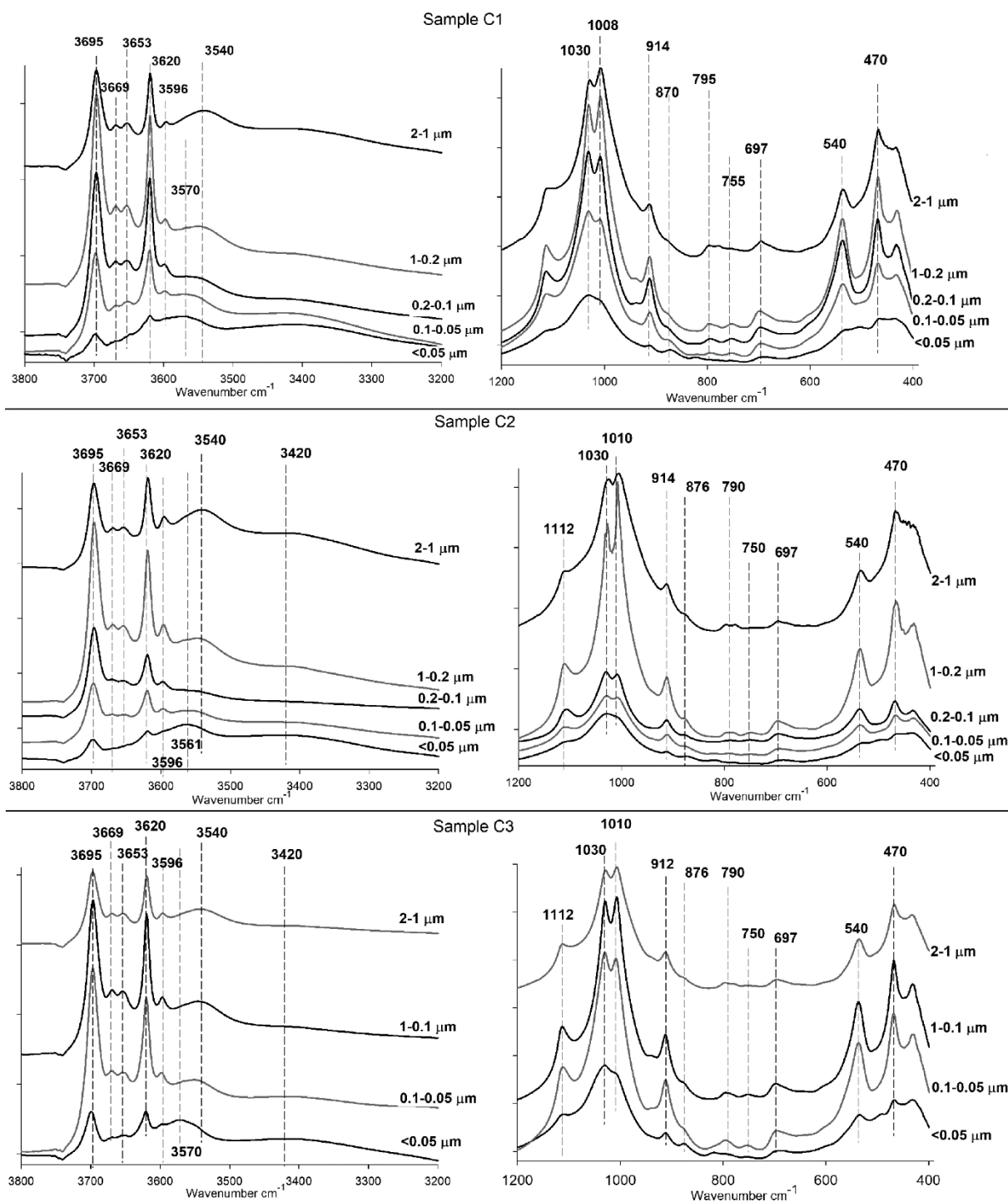


Figure 4 – MIR spectra for all samples

Chemical analyses by ICP-OES allowed determining the Cu associations in the <2 $\mu$ m sub-fractions. The results revealed that Cu contents are higher in the coarsest size fractions (Table 2), composed mainly of biotite as compared to the finest fractions composed especially of smectite. Unfortunately, the amounts of 0.05 to 1 $\mu$ m fractions for samples C2 and C3 were not sufficient to perform the ICP analysis.

Table 2 - Chemical analyses by ICP for sample C1 (weight %). ns - no sample

Sample	Cu (wt%)	Sample	Cu (wt%)	Sample	Cu (wt%)
C1 <2 $\mu\text{m}$	0.623	C2 <2 $\mu\text{m}$	0.78	C3 <2 $\mu\text{m}$	1.09
C1 <1 $\mu\text{m}$	0.471	C2 <1 $\mu\text{m}$	ns	C3 <1 $\mu\text{m}$	ns
C1 <0.2 $\mu\text{m}$	0.447	C2 <0.2 $\mu\text{m}$	ns	C3 <0.2 $\mu\text{m}$	ns
C1 <0.1 $\mu\text{m}$	0.265	C2 <0.1 $\mu\text{m}$	ns	C3 <0.1 $\mu\text{m}$	ns
C1 <0.05 $\mu\text{m}$	0.129	C2 <0.05 $\mu\text{m}$	0.71	C3 <0.05 $\mu\text{m}$	0.81

#### 4. DISCUSSION

In oxidized ores, Cu is frequently associated to goethite (Oliveira et al., 1995; Veiga et al., 1991; Gerth, 1990; Toledo-Groke et al., 1987; Ildefonse et al., 1986); however, in the Furnas deposit, this element is preferentially associated to cryptomelane, as observed by Mosser and Zeegers (1988) in Burkina Faso (Africa) and Traina and Doner (1985). The chemical analyses (Table 1) performed in this study also confirmed this assumption. Even though Fe-oxides/hydroxides represented from 40 to 55% (mass) of the samples, less than 0.1% of Cu is associated to them, according to the ICP analyses of the solutions from the DCB treatment. In fact, in the Furnas deposit, Cu is approximately partitioned as 50% in cryptomelane and 50% in the clay minerals. Concerning the clay minerals, biotite followed by mixed layers biotite/vermiculite or biotite/smectite exhibited the highest contents of Cu. Smectite (mainly nontronite) revealed the lowest Cu content (Table 2). FTIR from the clay fraction showed that copper is not associated to smectite as structural cation or as interlayer cation, since only 0.01 wt% of Cu is exchangeable, as also registered by Toledo-Groke et al., (1987).

Petit et al. (1992) showed that smectites from the Salobo deposit exhibited a nontronite composition. Furnas profile is a typical weathering profile found in the Carajás Province, similar to the Salobo deposit (Ildefonse et al., 1986; Toledo-Groke et al., 1987 and Veiga et al., 1991) and also resembling the Burkina Faso deposit (Africa) described by Mosser and Zeegers, (1988). The alteration processes were responsible for the dissolution of primary sulphides. The Cu released by sulfide dissolution is afterwards incorporated by biotites and vermiculites from the gneisses, according their schistosity (Toledo-Groke et al., 1987). The Cu-rich biotites altered to an interlayered clay mineral of 10-14 Å (biotite-smectite-vermiculite) and subsequently to an Al-Fe-Cu smectite (nontronite); finally, smectite was transformed into a kaolinite depleted in Cu.

#### 5. CONCLUSIONS

In the Furnas deposit, as well as in the Burkina Faso deposit, Cu is mainly assigned to cryptomelane instead of goethite, as observed at the Salobo deposit. Expressive Cu amounts were determined in interlayered clay minerals, possibly a biotite-vermiculite type. Unfortunately, the copper associated to clay minerals is not easy to recover, even in an acid leaching route; therefore, copper behavior in the weathering environment demands more studies in order to completely understand the geochemical fixing process in the lateritic minerals.

#### ACKNOWLEDGMENTS

This study has been supported by CNPq (Conselho Nacional de Desenvolvimento Científico e Tecnológico) - Project Ciências Sem Fronteiras: 249132/2013-3 and ITV – Instituto Tecnológico Vale. The authors also thank Elisabeth Fonseca and Antonio Clareti, geologist and engineer, respectively, from VALE. One of the authors, E. Mano acknowledges The Mineralogical Society of Great Britain and Ireland (Clay Minerals Group) for a student travel grant, which allowed her to present these results at the 16<sup>th</sup> International Clay Conference, held in Granada – Spain in July, 2017.



## REFERENCES:

- Dean, W.E Jr. (1974) Determination of carbonate and organic matter in calcareous sediments and sedimentary rocks by loss on ignition: comparison with other methods. *Journal of sedimentary petrology*. 44, 1, 242-248.
- Farmer, V.C. (1974) *Infrared spectra of minerals*. Mineralogical Society Monograph 4, Mineralogical Society, London.
- Gerth, J. (1990) Unit-cell dimensions of pure and trace metal-associated goethites. *Geochimica et Cosmochimica Acta*. 54, 363-371.
- Groves, D.I., Bierlein, F.P., Meinert, L.D. and Hitzman, M.W. (2010) Iron Oxide Copper-Gold (IOCG) Deposits through Earth History: Implications for Origin, Lithospheric Setting, and Distinction from Other Epigenetic Iron Oxide Deposits. *Economic Geology*. 105, 641–654.
- Ildelfonse, P., Manceau, A., Prost D. and Groke, M.C. T. (1986) Hydroxy-Cu-vermiculite formed by the weathering of Fe-biotites at Salobo, Carajás, Brazil. *Clays and Clay Minerals*. 34, 3, 338-345.
- Iriarte, I., Petit, S., Huertas, F.J., Fiore, S., Grauby, O., Decarreau, A. and Linares, J. (2005) Synthesis of kaolinite with a high level of Fe<sup>3+</sup> for Al substitution. *Clays and Clay Minerals*. 53, 1, 1-10.
- Laird, D. A., Barak, P., Nater, E. A., and Dowdy, R. H. (1991) Chemistry of smectitic and illitic phases in inter- stratified soil smectite: *Soil Sci. Soc. Am. J.* 55, 1499-1504.
- Madejová J., Balan E. and Petit S. (2011) Application of vibrational spectroscopy to the characterization of phyllosilicates and other industrial minerals. *EMU Notes in Mineralogy*. 9, 6, 171-226.
- Madejová J., Arvaiová, B. and Komadel, P. (1999) FTIR spectroscopic characterization of thermally treated Cu<sup>2+</sup>, Cd<sup>2+</sup>, and Li<sup>+</sup> montmorillonites. *Spectrochimica Acta Part A*. 55, 2467 - 2476.
- Mano, E. S., Caner, L. and Chaves, A. P. (2015) Metodology for lateríticos Cu-bearing clay minerals characterization. *Holos*. 31, 7, 3-12.
- Mehra, O.P. and Jackson, M.L. (1960) Iron oxide removal from soils and clays by a dithionite-citrate system buffered with sodium bicarbonate. *Clays and Clay Minerals*. 7, 317-327.
- Monteiro, L.V.S., Xavier, R.P., de Souza Filho, C.R. and Moreto, C.P.N. (2014) Metalogênese da Província Carajás. Org. Silva, M.G. da, Rocha Neto, M.B. da, Jost, H. and Kuyumjian, R.M: Metalogênese das províncias tectônicas brasileiras. CPRM – Companhia de Pesquisas de Recursos Minerais - Serviço Geológico do Brasil. Belo Horizonte, Minas Gerais. 43-92.
- Moreto, C.P.N., Monteiro, L.V.S., Xavier, R.P., Creaser, R.A., DuFrane, S.A., Tassinari, C.C.G., Sato, K., Kemp, A.I.S. and Amaral, W.S. (2015) Neoproterozoic and Paleoproterozoic Iron Oxide-Copper-Gold Events at the Sossego Deposit, Carajás Province, Brazil: Re-Os and U-Pb Geochronological Evidence. *Economic Geology*. 110, 809–835.
- Moore, D.M. and Reynolds, R.C.Jr. (1989) *X-ray diffraction and the identification and analysis of clay minerals*. University Press: Oxford.

- Mosser, C. and Zeegers, H. (1988) The mineralogy and geochemistry of two copper-rich weathering profiles in Burkina Faso, West Africa. *Journal of Geochemical Exploration*. 30, 145-166.
- Oliveira, S.M.B. de, Carvalho e Silva, M.L.M. de, Toledo, M.C.M de (1995) The role of residual 2:1 phyllosilicates in lateritic metallogenesis: Ni and Cu deposits in Serra dos Carajás, Brazilian Amazonia. *Geochim. Brasil*. 9, 2, 161-171.
- Petit, S., Decarreau, A., Gates, W., Andrieux, P. and Grauby, O. (2015) Hydrothermal synthesis of dioctahedral smectites: The Al-Fe<sup>3+</sup> chemical series. Part II: Crystal-chemistry. *Applied Clay Science* 104, 96–105.
- Petit, S., Decarreau, A., Mosser, C., Ehret, G. and Grauby, O. (1995) Hydrothermal synthesis (250°C) of copper-substituted kaolinites. *Clays and Clay Minerals*. 43, 4, 482-494.
- Petit, S., Prot, T., Decarreau, A., Mosser, C. and Toledo-Groke, M.C. (1992). Crystallochemical study of a population of particles in smectites from a lateritic weathering profile. *Clays and Clay Minerals*. 40, 4, 436-445.
- Petit, S. and Decarreau, A. (1990) Hydrothermal (200°C) synthesis and crystal chemistry of iron-rich kaolinites. *Clay Minerals*. 25, 181-196.
- Schwarz, M. and Frantz, J. (2013) Depósito de Cu-Zn Pojuca Corpo Quatro: IOCG ou VMS? *Pesquisas em Geociências*. 40, 1, 5-19.
- Seiffarth, T. and Kaps, C. (2009) Structural characterization of (Cu<sup>2+</sup>, Na<sup>+</sup>) and (Cu<sup>2+</sup>, NH<sup>4+</sup>) exchanged bentonites upon thermal treatment. *Clays and Clay Minerals*. 57, 1, 40–45.
- Tallarico, F.H.B., Figueiredo, B.R., Groves, D.I., Kositcin, N., Mcnaughton, N.J., Fletcher, I.R. and Rego, J.L. (2005) Geology and SHRIMP U-Pb Geochronology of the Igarapé Bahia Deposit, Carajás Copper-Gold Belt, Brazil: An Archean (2.57 Ga) Example of Iron-Oxide Cu-Au-(U-REE) Mineralization. *Economic Geology*. 100, 7–28.
- Teixeira, J.B.G.; Lindenmayer, Z.G. and Da Silva, M. da G. (2010) Depósitos de óxidos de ferro-cobre-ouro de Carajás. In: *Modelos de depósitos de cobre do Brasil e sua resposta ao intemperismo*. De Brito, R.S.C.; Da Silva, M. da G. and Kuyumjian, R.M. (Ed.) – Programa Geologia do Brasil: Recursos Minerais – série metalogenia. CPRM – Serviço Geológico do Brasil. 11-213.
- Toledo-Groke, M.C., Melfi, A.J. and Parisot, J.C. (1987) Comportamento do cobre durante o intemperismo das rochas xistosas cupríferas do Salobo 3α, Serra dos Carajás. *Geochimica Brasiliensis*. 1, 2, 187-200.
- Traina, S.J. and Doner, H.E.. (1985) Co, Cu, Ni, and Ca sorption by a mixed suspension of smectite and hydrous manganese dioxide. *Clays and Clay Minerals*. 33, 2, 118-122.
- Veiga, M.M., Schorscher, H.D. and Fyfe, W.S. (1991) Relationship of copper with hydrous ferric oxides: Salobo, Carajás, PA, Brazil. *Ore Geology Reviews*. 6, 245-255.